Plant Physiology and Biochemistry 143 (2019) 340–350

Contents lists available at ScienceDirect

Plant Physiology and Biochemistry

journal homepage: www.elsevier.com/locate/plaphy

Research article

Functional identification of *Ammopiptanthus mongolicus* anion channel AmSLAC1 involved in drought induced stomata closure

Li Junlin[a,d,1], Han Lei[b,c,1], Su Yanhua[c], Guo Hongen[a], Zhang Huanchao[d,e,*]

[a] Shandong Institute of Sericulture, Yantai, 264002, China
[b] Lu Dong University, Yantai, 264025, China
[c] State Key Laboratory of Soil and Sustainable Agriculture, Institute of Soil Science, Chinese Academy of Sciences, Nanjing, 210008, China
[d] College of Forestry, Nanjing Forestry University, Nanjing, 210037, China
[e] Co-Innovation Center for the Sustainable Forestry in Southern China, Nanjing Forest University, Nanjing, 210037, China

ARTICLE INFO

Keywords:
S-type anion channel
Ammopiptanthus mongolicus
Stomatal closure
Drought

ABSTRACT

Drought, one of the most acute abiotic stressors plants encountered, can adversely affect plants growth and development. The fast adjustment of stomatal aperture is necessary for effective drought tolerance in plants. Anion channels were identified as important controllers of stomatal closing via mediating anion efflux. The present study reports the isolation and identification of a SLAC (SLOW ANION CHANNEL-ASSOCIATED 1) ortholog from an ancient desert shrub *Ammopiptanthus mongolicus* (Maxim.) Cheng f. (AmSLAC1), which is functionally conserved for ABA and drought induced stomata closure. *AmSLAC1* was primarily expressed in shoots, especially in guard cells. The transcription of *AmSLAC1* was induced in response to ABA and PEG treatments, implying the potential involvement in ABA-induced drought stress responses. Fluorescence observation suggested that AmSLAC1 was localized in the plasma membrane. BiFC asssays demonstrated an interaction between AmSLAC1 and the typical calcium-dependent protein kinases AmCPK6. Ectopic expression of *AmSLAC1* restores a *slac1*-defective phenotype in Arabidopsis. Furthermore, anion conductance mediated by AmSLAC1 can be activated by AmCPK6 in *Xenopus oocytes*. Taken together, these results demonstrate that the expression of *AmSLAC1* enables the complement of the phenotypes of Arabidopsis *slac1* mutants, indicating that AmSLAC1, as an anion channel and regulated by AmCPK6, is functionally conserved for ABA and drought induced stomata closure.

1. Introduction

Drought, one of the most acute abiotic stressors plants encountered, can adversely affect plants growth and development (Bechtold, 2018; Hussain et al., 2018). Over the course of evolution, plants have developed sophisticated mechanisms that allow adaptation and survival during periods of water deficit (Bhargava and Sawant, 2013). The maintenance of water absorption mediated via modulation of root architecture, and water loss is also limited through reducing stomatal conductance and evaporative surfaces. The fast adjustment of stomatal aperture is necessary for effective drought tolerance in plants (Jezek and Blatt, 2017; Zoulias et al., 2018). The release of osmoregulatory ions (K^+, Cl^-, and malate^{2-}) from guard cells reduces its osmotic potential and results in stomatal closure.

Anion channels were identified as important controllers of stomatal closing via mediating anion efflux. Two major types of anion channels have been characterized in the plasma membrane: S-type anion channels and R-type anion channels according to electrophysiological properties (Schroeder and Keller, 1992). SLAC1 (SLOW ANION CHANNEL-ASSOCIATED 1) was originally cloned from Arabidopsis and regarded as guard cell anion channel in plants, which was activated by various physiological and stress stimulis, including increased [CO_2], ozone, drought hormone ABA, light/dark transitions, humidity change, Ca^{2+}, H_2O_2, NO and flagellin, and lead to stomata closure (Negi et al., 2008; Vahisalu et al., 2008, 2010; Brandt et al., 2012; Laanemets et al., 2013; Guzel Deger et al., 2015). Isolated by an infrared thermography camera, a SLAC1-deficient mutant of rice had significantly higher stomatal conductance, rates of photosynthesis, and rations of internal [CO_2] to ambient [CO_2] compared with wild-type plants (Kusumi et al., 2012). Moreover, the dominant-positive mutant OsSLAC1-F461A had a 70% reduction of stomatal conductance compared with the WT plants (Kusumi et al., 2017). Qi et al. (2018) identified the gene encoding

* Corresponding author. NO. 159 Longpan Road, Nanjing, 210037, Jiangsu Province, PR China.
E-mail address: hczhang@njfu.edu.cn (Z. Huanchao).
[1] These authors contributed equally to this work.

https://doi.org/10.1016/j.plaphy.2019.09.012
Received 4 July 2019; Received in revised form 6 September 2019; Accepted 6 September 2019
Available online 06 September 2019
0981-9428/

ZmSLAC1 in maize, and the maize mutants *zmslac1-1* and *zmslac1-2* with a mutator transposon in ZmSLAC1 exhibited strong insensitive phenotypes of stomatal closure in response to diverse stimulis.

Ammopiptanthus mongolicus (Maxim.) Cheng f. Is an endangered fabaceous shrub growing in desert or semi-desert areas in the northwest of China (Gao et al., 2015; Jin et al., 2018). They survive the persistent stresses of an extremely arid atmosphere and water shortage, which makes them useful in maintaining the sustainability of desert ecosystems. In the present study, we isolated and characterized the function of AmSLAC1 from *Ammopiptanthus mongolicus* (AmSLAC1) and demonstrated its physiological roles by transgenic analysis in Arabidopsis and electrophysiology analysis. The results showed that the expression of AmSLAC1 enables the complement of the phenotypes of Arabidopsis *slac1* mutants, indicating that AmSLAC1, as an anion channel and regulated by AmCPK6, is functionally conserved for ABA and drought induced stomata closure.

2. Methods and materials

2.1. Plant growth

Ammopiptanthus mongolicus seeds were collected from a single shrub grown in Min Qin Desert Botanical Garden, Gansu, China. These seeds were surface-sterilized with Clorox solution and soaked in water for 2 days at 26 °C. Seeds were germinated on moist filter paper and placed in sterile petri dishes for 3–4 days. Seedlings were then transferred to half strength Hoagland solution in a greenhouse at approximately 26 °C with a photoperiod of 16 h light and 8 h dark for 4 weeks. After that the seedlings were divided into several groups. The first group served as control sample, the others were transferred to half strength Hoagland solution containing 18% PEG (~ −0.4 MPa) or 100 μM ABA (Sigma). The shoots were harvested separately at different time points (0, 1, 3, 6, 12, 24 or 48 h) and then frozen in liquid nitrogen immediately.

2.2. DNA and RNA preparation and cDNA synthesis

The total genomic DNA of the *Ammopiptanthus* was extracted by applying cetyltrimethylammonium ammonium bromide (CTAB). Total RNA of the *Ammopiptanthus* samples were isolated by using TRIzol total RNA extraction kit (Invitrogen, USA) according to the manufacturer's protocol. According to the manufacturer's instructions, the first-strand cDNAs were synthesized through a PrimeScript™ RT reagent Kit, gDNA Eraser (TAKARA, Japan) and oligo (dT) primers.

2.3. Real-time PCR

For Real-Time Quantitative RT-PCR, PCR amplification was performed in a 20 μL reaction system containing 2.5 μL of 5 x diluted cDNA templates, 0.2 μM of each forward and reverse primers and 10 μL SYBR Green PCR Master Mix (TAKARA, Japan). The reaction was performed with CFX96TM Real-Time PCR cycler programmed with: 45 cycles of 95 °C for 15 s, 60 °C for 15 s and 72 °C for 15 s. Specific primers (Forward: 5′- ATAAGCAAGGGCCTTGCTATTGGT -3′, Revese: 5′ TGAC TTGAATCCTTGTTCAC′) of *AmSLAC1* were used, and *AmEIF1* (Forward: 5′- CTGACATGCGCCGTAGGAACG-3'; Reverse: 5′-CCCTGCTTATGCCA GTCTTTT-3′) was used as a reference (Shi et al., 2012). The threshold cycle (CT) values were used to calculate the fold-change of relative expression with formula $2^{-\Delta\Delta CT}$ and the standard error. Three biological replicates were analyzed for every treatment, and each reaction in technical triplicate to reduce the error.

2.4. Cloning

Based on a previous transcriptomic analysis (Jin et al., 2018), a partial *AmSLAC1* sequence was initially identified according to the sequence of *SLAC1* in Arabidopsis. According to the partial *AmSLAC1* sequence, the primer of AmSLAC1-R (5′- TCATTCTTGACTTGAATCC TTG -3′) was designed for 5′ RACE using the SMARTer RACE cDNA Amplification Kit (Takara, Japan). For the nested PCR, the 5′RACE reactions were performed as follows: pre-denaturation at 95 °C for 3 min; 5 amplification cycles (denaturation at 95 °C for 30 s, elongation at 72 °C for 3 min), then 27 amplification cycles (denaturation at 95 °C for 30 s, annealing at 65 °C for 30 s, elongation at 72 °C for 3 min) with a final extension for 10 min at 72 °C. The full length of *AmSLAC1* was amplified by the primers AmSLAC1-R and AmSLAC1-F (Supplemental Table 1), which were designed based on the results of 5′RACE with the cDNA of *Ammopiptanthus mongolicus*. The PCR products were analyzed by electrophoresis on a 1% agarose gel. The target bands were purified and ligated into the pEasy-Blunt zero vector (Transgen Biotech) for sequencing.

The cloning of *AmCPK6* was conducted according to method as described as *AmSLAC1*, and submitted to GeneBank (GenBank accession: KT851555.1 for *AmCPK6*).

Promoter sequence of *AmSLAC1* was cloned according to Liu (Liu and Chen, 2007) and the method we reported above (Han et al., 2018). Three specific reverse primers (AmSLAC-SP3, AmSLAC-SP2 and AmSLAC-SP1) were designed according to the 5′-region of *AmSLAC1* genomic DNA sequence. Four arbitrary degenerate primers were used as forward primers in the first hi-TAIL-PCR. The AC1 primer was used in the secondary and third hi-TAIL-PCR. The primers sequences are listed in Supplementary Table 1. After three rounds of hi-TAIL-PCR, a long of 1455 bp sequence above ATG of *AmSLAC1* was isolated and designed as promoter region of *AmSLAC1*, and subsequently submitted to GeneBank (GenBank accession: KT851557.1).

2.5. Histochemical GUS staining

Using the specific primers AmSLAC1pro-F and AmSLAC1pro-R (Supplementary Table 1), which contained *Sac* I and *Nco* I specific restriction endonuclease enzyme sites respectively, to amplify the promoter sequence of *AmSLAC1*. The PCR products was subcloned into pEasy-Blunt zero vector (Transgen Biotech). To construct the transgenic vector pCambia1301-Pro*AmSLAC1*-GUS, the 35S promoter of the *GUS* reporter gene was replaced by the promoter of *AmSLAC1* from the pEasy -Pro*AmSLAC1* via *Sac* I and *Nco* I restriction sites. The resulting construct was introduced into Agrobacterium strain *GV*3101, which served as an intermediate for transforming *AmSLAC1* promoter into wild-type Arabidopsis plants. Transgenic plants were selected on 1/2 MS (Murashige and Skoog, 1962) media containing 50 mg/L hygromycin. The antibiotic-resistant plants were initially identified by PCR analysis which uses the primers of AmSLAC1pro-F and AmSLAC1pro-R (Supplemental Table 1) and genomic DNA as template.

The T_3 seedlings of *ProAmSLAC1*::*GUS* transgenic plants were used to determine the GUS staining as previously described (Han et al., 2018). Briefly, seedlings were immersed in staining solution (2 mM 5-bromo-4-chloro-3-indolyl-β-D-glucuronide, 2 mM $K_3Fe(CN)_6$, 2 mM $K_4Fe(CN)_6$, and 0.2% (*v*/*v*) Triton X-100, 50 mM sodium hydrogen phosphate buffer solution, pH7.2) and vacuum-infiltrated for 15 min in a vacuum desiccators. The samples were then incubated in the staining solution at 37 °C for 14 h, the staining solution was removed and the samples were washed with 25%, 50%, 75% ethanol for two times to remove the chlorophyll. The images were taken under a dissecting microscope (Nikon).

2.6. Subcellular localization analysis

The CDS of *AmSLAC1,* without the termination codon, was amplified by using the specific primers AmSLAC1-F and AmSLAC1-R which contained *Xho* I and *Kpn* I specific restriction endonuclease enzyme sites respectively. The PCR products were cloned into pEasy-Blunt zero vector (Transgen Biotech), and subsequently fused with the GFP by subcloning into the plant expression vector pCambia 1300-GFP. The

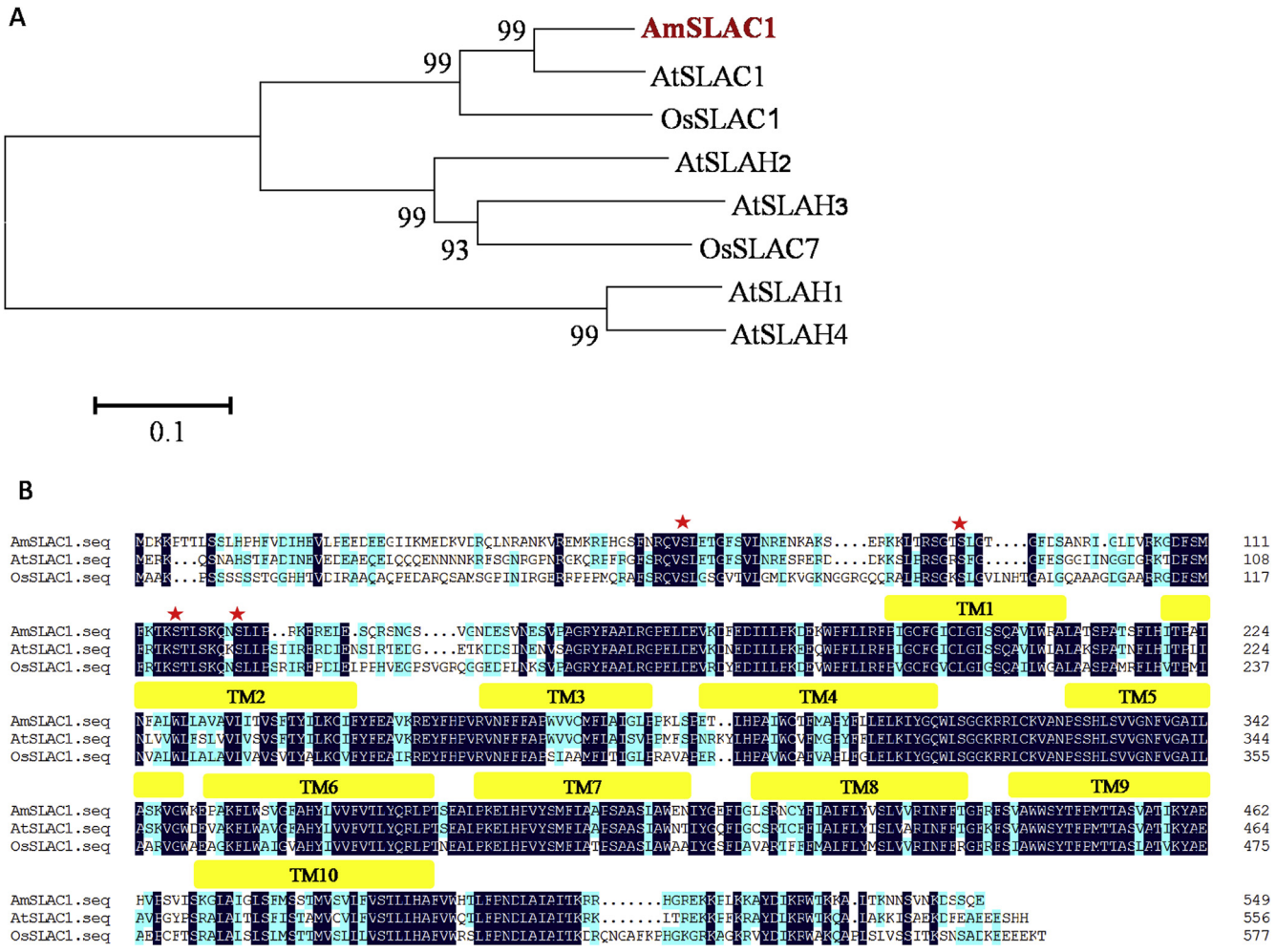

Fig. 1. Phylogenetic analysis and alignment of AmSLAC1 homologs. A. Phylogenetic tree of SLAC1 proteins from *Ammopiptanthus* and model plants Arabidopsis and rice. The Phylogenetic tree of SLAC1 was constructed with neighbor-joining method in MEGA 6.0 software program. The numbers beside each node represent bootstrap values based on 1000 replications. The scale bar indicates the relative amount of change along branches. AmSLAC1 (KT851554), AtSLAC1 (At1g12480), AtSLAH1 (At1g62280), AtSLAH2 (At4g27970), AtSLAH3 (At5g24030), AtSLAH4 (At1g62262), OsSLAC1 (XP_015636891.1), OsSLAC7 (Os01g28840.1). B. Sequences aligned are from the SLAC1 homologs of *Ammopiptanthus* and model plants Arabidopsis and rice. The black, blue and white backgrounds indicate perfect (100%), intermediate (50%) and low (33%) identities respectively. The amino acids (S62, S89, S116 and S123) marked by the red stars are the conserved residues involved in the phosphorylation. . (For interpretation of the references to colour in this figure legend, the reader is referred to the Web version of this article.)

fusion vector pCambia1300-AmSLAC1-GFP and the control vector pCambia1300 were used for transient expression in Arabidopsis protoplast cells as described previously (Han et al., 2018). The constructed plasmids were transformed into Agrobacterium strain *GV*3101, which was infiltrated in *Nicotiana benthamiana* leaves. GFP fluorescence was visualized with a Zeiss LSM710 confocal laser microscope (Carl Zeiss, Germany) by using excitation with a 488 nm laser.

2.7. Construction of transgenic plant lines

The CDS of *AmSLAC1* was amplified by primers AmSLAC1-GW-F and AmSLAC1-GW-R (Supplemental Table 1), and then the PCR product was cloned into pDONR222 vector via BP Clonase™ II Enzyme Mix (Life technologies, Shanghai) following the manufacturer's instructions. To generate the AmSLAC1-pGreen-35S construction, AmSLAC1-pDNOR222 clone was digested by Xho *I* and recombined with the pGreen-35S vector by LR Clonase™ II Enzyme Mix (Life technologies, Shanghai). The AmSLAC1-pGreen-35S vector was introduced into Agrobacterium strain *GV*3101, which served as an intermediate for transforming *AmSLAC1* into *slac1 loss of function mutants (slac1-3)* or wild-type Arabidopsis plants. Transgenic plants were selected on 1/2 MS (Murashige and Skoog, 1962) media containing 50 mg/L hygromycin. The antibiotic-resistant plants were initially identified by PCR analysis that uses the primers of AmSLAC1-GW-F and AmSLAC1-GW-R (Supplemental Table 1) and genomic DNA as template. The T_3 seedlings were used for further studies.

Analysis of the leaf water loss rate.

Leaf water loss analysis was conducted as described previously (Han et al., 2018). Rosette leaves were detached from 4-week-old plants and immediately weighed (W_0). The weight (W_t) was recorded at the designated time intervals (0, 30, 60, 90, 120, 180, 240, 300 min after detachment) at 23 °C with an RH of 70% in growth room. The water loss rates were calculated as $(W_0\text{-}W_t)/W_0$. The experiments were repeated 3 times, each time with three replicate leaves per line.

2.8. Stomatal aperture measurements

Stomatal aperture measurements were conducted as previously described (Han et al., 2018). 4-week-old rosette leaves were used for stomatal measurements. Epidermal strips were maintained in opening buffer (10 mM KCl, 10 mM MES, adjust pH to 6.15 with TRIS) for 3 h under light (120 μmol/m^2/s) to induce stomatal opening. The leaves were incubated for an additional 2 h in the presence or absence of ABA (10 μM). The epidermal peels were examined under a 40× objective

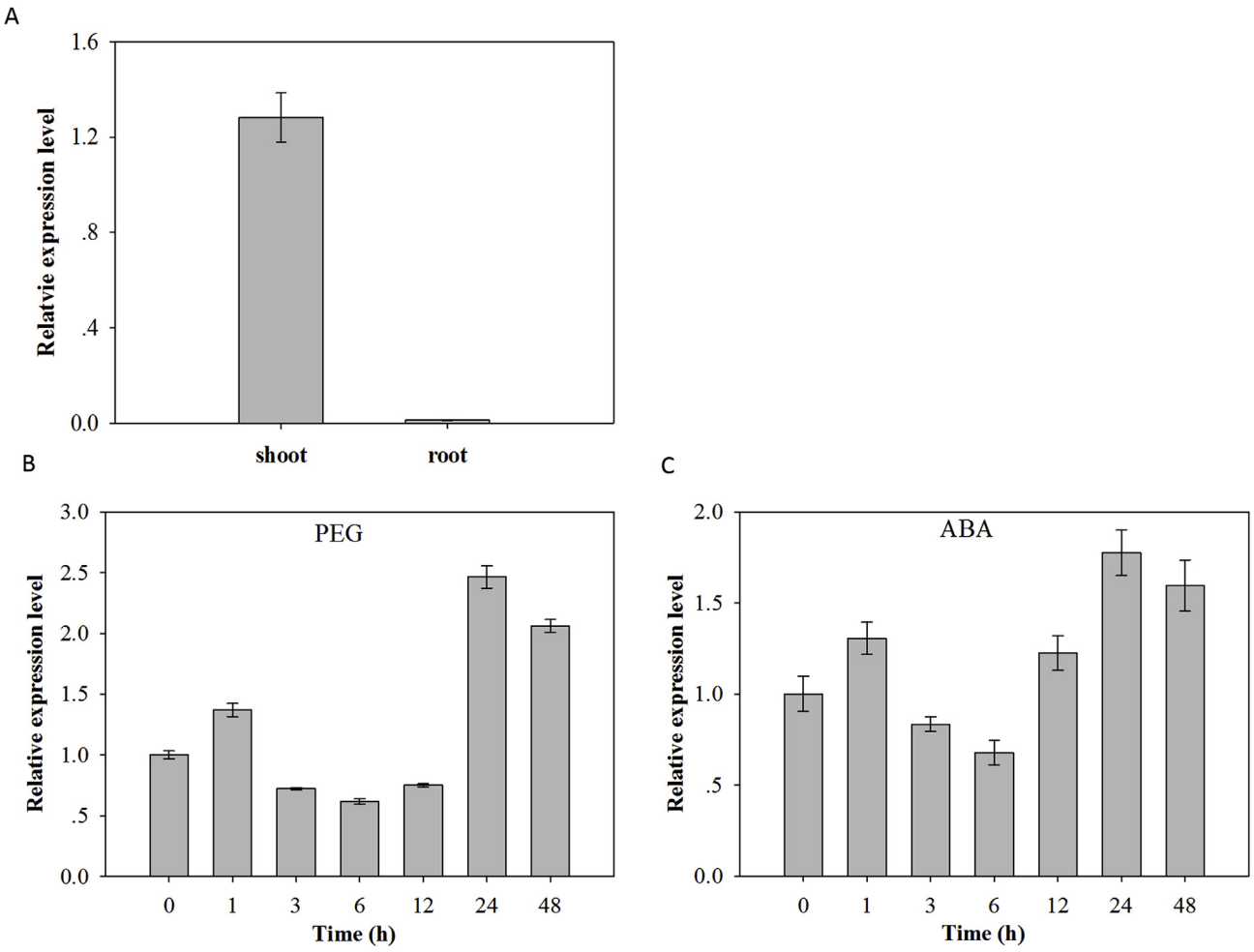

Fig. 2. Expression analysis of *AmSLAC1*. A. Transcript levels of *AmSLAC1* were evaluated in shoots and roots by real-time quantitative RT-PCR. Four-week-old seedlings were transferred to hydroponic medium supplemented with 18% PEG (*m/v*) (B) or 100 μM ABA (C) followed by transcript measurements in shoots. Transcripts of *AmSLAC1* were measured by quantitative RT-PCR and normalized to the *AmEIF1* gene in control seedlings grown under stress-free conditions. The threshold cycle (CT) values were used to calculate the fold-change of relative expression with formula $2^{-\Delta\Delta CT}$ and the standard error. Three biological replicates were analyzed for every treatment, and each reaction in technical triplicate to reduce the error.

using a light microscope (Nikon, Ti–S). After image acquisition, the widths of the stomatal apertures were measured by ImageJ software (National Institutes of Health). Three replicates (120 stomata from one seedling per replicate) were used for one experiment, and at least three independent experiments were conducted.

2.9. Gas exchange characteristics

Photosynthesis, stomatal conductance and transpiration rate were measured by a portable photosynthesis system (LICOR6400, Li-Cor, Inc., Lincoln, NE, USA). The measurements were made on the middle portion of the third leaf of seedlings between 10:00 and 13:00. The leaf cuvette environment was controlled at a photosynthetically active radiation (PAR) of 1000 μmol/m^2/s, relative humidity of 70%, leaf temperature of 23 °C, and [CO_2] of 400 ppm.

2.10. BiFC assay

BiFC assay was carried out as described previously (Han et al., 2018). *AmSLAC1* was cloned into gateway compatible BiFC vector pEarleyGate201-YN, *and AmCPK6* was cloned into vector pEarleyGate202-YC. The constructed plasmids were co-transformed into Agrobacterium strain *GV*3101. Pairs of combinations were co-infiltrated in *Nicotiana benthamiana* leaves and analyzed by biomolecular fluorescence complementation (BiFC) assays. At 48–72 h after infiltration, the YFP signal was observed by confocal laser scanning microscopy (Zeiss, LSM710). The results were repeated at least three times.

2.11. Heterologous expression in Xenopus oocytes

The CDS of *AmSLAC1* was cut out from pEasy–AmSLAC1, and subcloned into the *Xho* I and *Not* I sites of pCI vector to yield the final plasmid pCI-AmSLAC1 for TEVC. CDS of *AmCPK6* was amplified from *A. mongolicus* cDNA and cloned into pCI vector. Oocytes were injected with 50 nL of co-expressing plasmids (1.5 μg/μL) or 50 nL sterilized water for control, and then kept at 20 °C for 2 days supplemented with 50 mg/L of gentamicin. For anion channel current recording, the standard bath solution contained 75 mM NaCl, 1 mM $CaCl_2$, 1 mM $MgCl_2$, 57 mM D-sorbitol and 10 mM Hepes-Tris (pH 7.4), were used. Whole-oocytes currents were recorded by using a step voltage protocol with 4 s voltage pulses from +40 to - 140 mV with a 10 mV decrement, and the holding potential was −40 mV. The channel currents were recorded by a pCLAMP 10.0 (Axon) connected to a personal computer. Glass pipettes were filled with 3 M KCl as pipette solution.

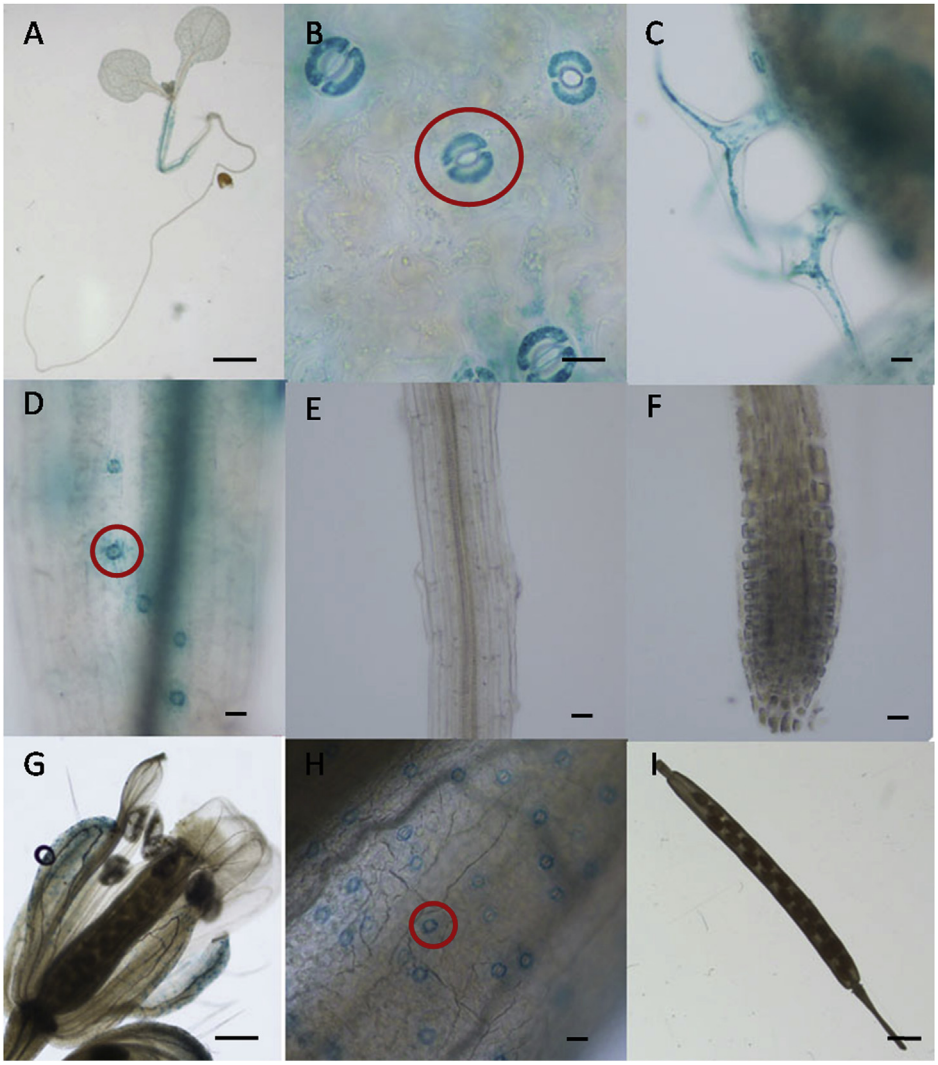

Fig. 3. Tissue localization pattern of *AmSLAC1* in transgenic Arabidopsis. A, distinct GUS staining in hypocotyls of 6-day old seedlings; B, strong GUS activity in guard cells of cotyledon; C, strong GUS activity in trichomes; D, GUS signal in guard cells of hypocotyl; no apparent GUS staining in roots (E) and (F); G, inflorescences; strong GUS activity in guard cells of sepal (H), and no signals in silique (I). Bars = 1 cm in (A) and (I), 10 μm in (B), (C), (D), (E), (F) and (H), 100 μm in (G).

3. Results

3.1. Isolation of a SLAC1 gene from Ammopiptanthus mongolicus

A partial *AmSLAC1* sequence (for a putative *A*mmopiptanthus *m*ongolicus *S*low *A*nion *C*hannel-Associated *1*) was identified from our RNA-seq profile based on its sequence homology with *Arabidopsis thaliana* SLAC1, and a 1792 bp full length *AmSLAC1* cDNA was amplified by RACE in the *Ammopiptanthus mongolicus* cDNA library. The primers AmSLAC1-F and AmSLAC1-R were designed to clone the gene in the *Ammopiptanthus mongolicus* cDNA and the genomic DNA to confirm the full length *AmSLAC1* sequence. A comparison of cDNA and genomic DNA sequences showed that *AmSLAC1* had 3 exons. The entire *AmSLAC1* ORF was 1650 bp long (GenBank accession: KT851554), encoding a predicted protein of 549 amino acids with a molecular mass of 62.142 kDa and an isoelectric point of 9.55.

A BLAST search in the NCBI protein database was performed to examine potential orthologs of AmSLAC1 in model plant species (Arabidopsis and rice). The closest homologue of AmSLAC1 in Arabidopsis is AtSLAC1 (At1g12480) and OsSLAC1 (XP_015636891.1) in rice (Fig. 1A). The amino acid sequence alignment of these three SLAC1 proteins showed that AmSLAC1 protein had higher similarity with AtSLAC1 than OsSLAC1 (71.9% identity with AtSLAC1; 61.6% identity with OsSLAC1) (Fig. 1B). Amino acid sequence of AmSLAC1 was comprised of 10 transmembrane region (Fig. 1B), in addition, several phosphorylation sites reported in Arabidopsis SLAC1, such as S59, S86, S113, and S120 (Geiger et al., 2010; Vahisalu et al., 2010), were all conserved in rice SLAC1 (Kusumi et al., 2012) as well as in *Ammopiptanthus mongolicus* SLAC1 (Fig. 1B), suggesting that AmSLAC1 protein may be activated by phosphorylation.

3.2. Expression analysis of AmSLAC1

To investigate the expression profile of *AmSLAC1*, qRT-PCR experiments were performed. As shown in Fig. 2A, the transcripts of *AmSLAC1* were restricted to the green parts of *Ammopiptanthus mongolicus* seedlings. In order to further detect the spatial expression pattern of *AmSLAC1* in more details, we cloned a 1456 bp promoter region (the DNA sequence above translation start of *AmSLAC1* CDS) of *AmSLAC1* by thermal asymmetric interlaced PCR (TAIL-PCR) (Liu and Chen, 2007) and the sequence was submitted to GeneBank (accession number: KT851557).

In general consistence with the shoot expressed *SLAC1* gene of Arabidopsis (Negi et al., 2008), the transgenic lines containing the

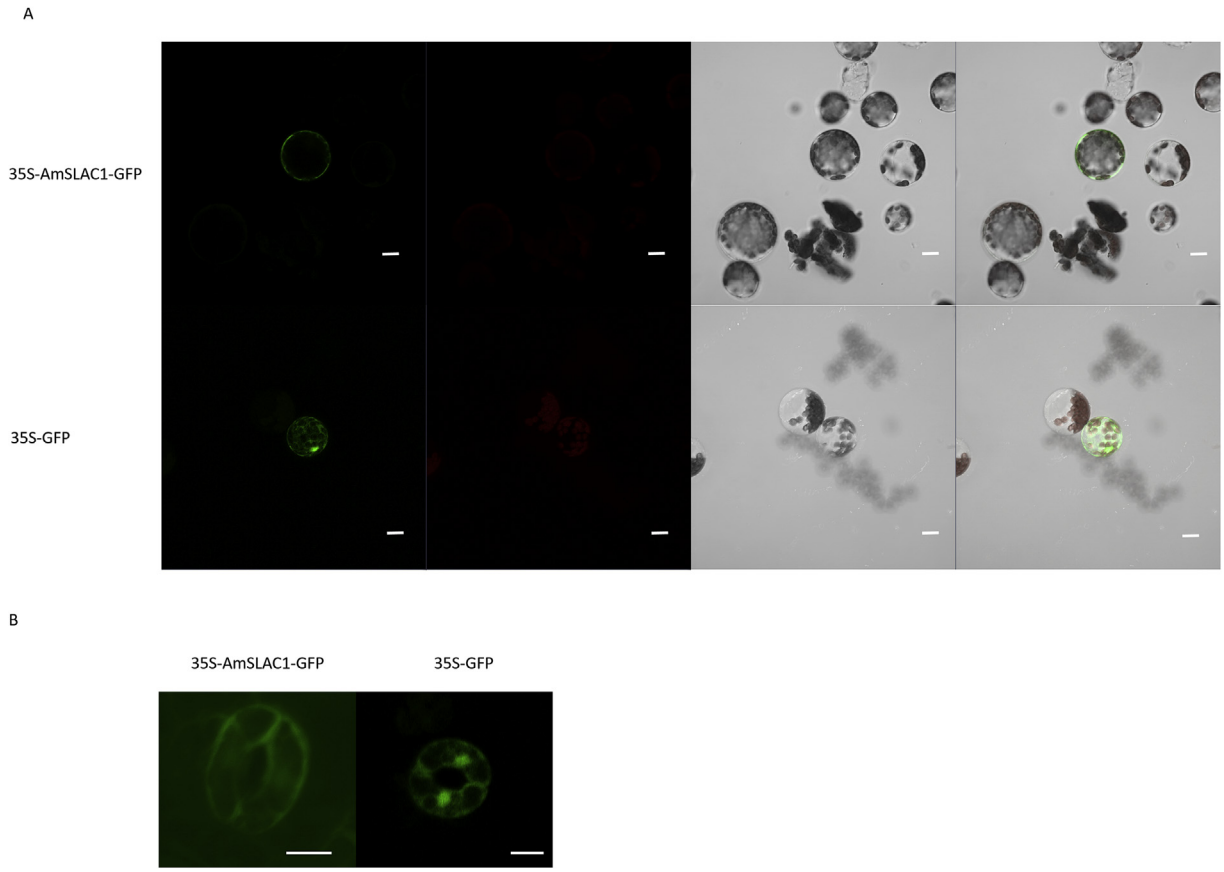

Fig. 4. Subcellular localization analysis of AmSLAC1 protein. (A) Arabidopsis mesophyll protoplast cells containing 35S:*AmSLAC1-GFP* (upper panel) and 35S: *GFP* (bottom panel) fusion genes were observed. (B) *Nicotiana benthamiana* guard cell. Scale bar = 10 μm.

Pro$_{AmSLAC1}$:*GUS* construct were used to determine the *GUS* expression. Results showed that high GUS signals were accumulated in the shoot including hypocotyl (Fig. 3A and D), guard cells of cotyledons (Fig. 3B) and sepals (Fig. 3G and H), but not in the root (Fig. 3E and F), which was in accordance with qRT-PCR results. The staining was also observed in the trichomes of leaves (Fig. 3C).

To investigate the response of *AmSLAC1* to drought stresses, we examined the *AmSLAC1* transcript abundance under PEG [18% (*m/v*)] or ABA (100 μM) in *Ammopiptanthus mongolicus* shoots. As showed in Fig. 2B, 4-h persistent stresses to the roots lead to strong induction (2.5 fold increases as compared to the initial abundances) of *AmSLAC1* expression by PEG treatment in shoots. The stimulation of *AmSLAC1* transcription under ABA treatment, to certain degree, coincided with that induced by PEG, was gradually increased and reached peak at the 24th hour, the increasing range is approximately 2-fold (Fig. 2C).

3.3. Subcellular localization of AmSLAC1

To analyze the subcellular localization of AmSLAC1, the transiently expressed plasmid of pCambia 1300-AmSLAC1-GFP was delivered into Arabidopsis mesophyll protoplasts. The empty vector pCambia1300-GFP was used as control. Observation of fluorescence showed that the AmSLAC1 protein was localized along cell outline (Fig. 4A). In addition, AmSLAC1-GFP was also infiltrated in *Nicotiana benthamiana* leaves. In accordance with that in mesophyll protoplasts, AmSLAC1-GFP signal was also showed along the guard cell outline (Fig. 4B), in contrast, the GFP signal was distributed throughout the cell in the *35S::GFP* construct, indicating that pCambia1300-AmSLAC1-GFP probably localizes in plasma membrane.

3.4. Ectopic expression of AmSLAC1 restores a slac1-defective phenotype in Arabidopsis

To explore the physiological function of *AmSLAC1 in planta*, we expressed *AmSLAC1* in *slac1* loss of function mutants (*slac1-3*) (Negi et al., 2008; Vahisalu et al., 2008). Twenty independent transgenic lines were identified. Real time RT-PCR analysis demonstrated that the expression of *AmSLAC1*, scarcely detected in *slac1-3* mutants, was strongly increased in the complementation lines *slac1/AmSLAC1* (Fig. 5A). Two representative lines COM1-3#1 and COM1-3#5 complemented for *slac1-3* were used in the following experiments. Firstly, we detected the leaf water loss rate in the wild-type, *slac1* mutants and the complementation lines *slac1/AmSLAC1*. The rosette leaves of those plants were excised and their fresh weight was measured at indicated time point. Over all, AmSLAC1 could reduce water loss from excised leaves to the extent of wild type (Fig. 5B). Water loss from detached *slac1* mutant leaves resulted in 64% fresh weight loss after 300 min, whereas in the wild type and complementation lines, fresh weight loss was no more than 45% after 300 min (Fig. 5B). Besides, there was not significant variation in stomatal density in either wild type, *slac1* mutants or complementation plants leaves (Fig. 5C). To further support this observation in *planta*, we examined whether the complementation lines confer dehydration stress tolerance. Wild type, *slac1-3* mutants and complementation lines were grown in pots for 4 weeks under normal condition, and then withheld watering for water deficit stress to further analyze drought tolerance. After two weeks, *slac1-3* mutants exhibited inhibitory growth state and severer chlorosis, whereas wild-type and transgenic plants remained healthier and greener, showing more vigorous inflorescences and siliques (Fig. 5D).

Since ABA play important roles in regulating stomatal movement, we used isolated epidermal peels to investigate the stomatal responses

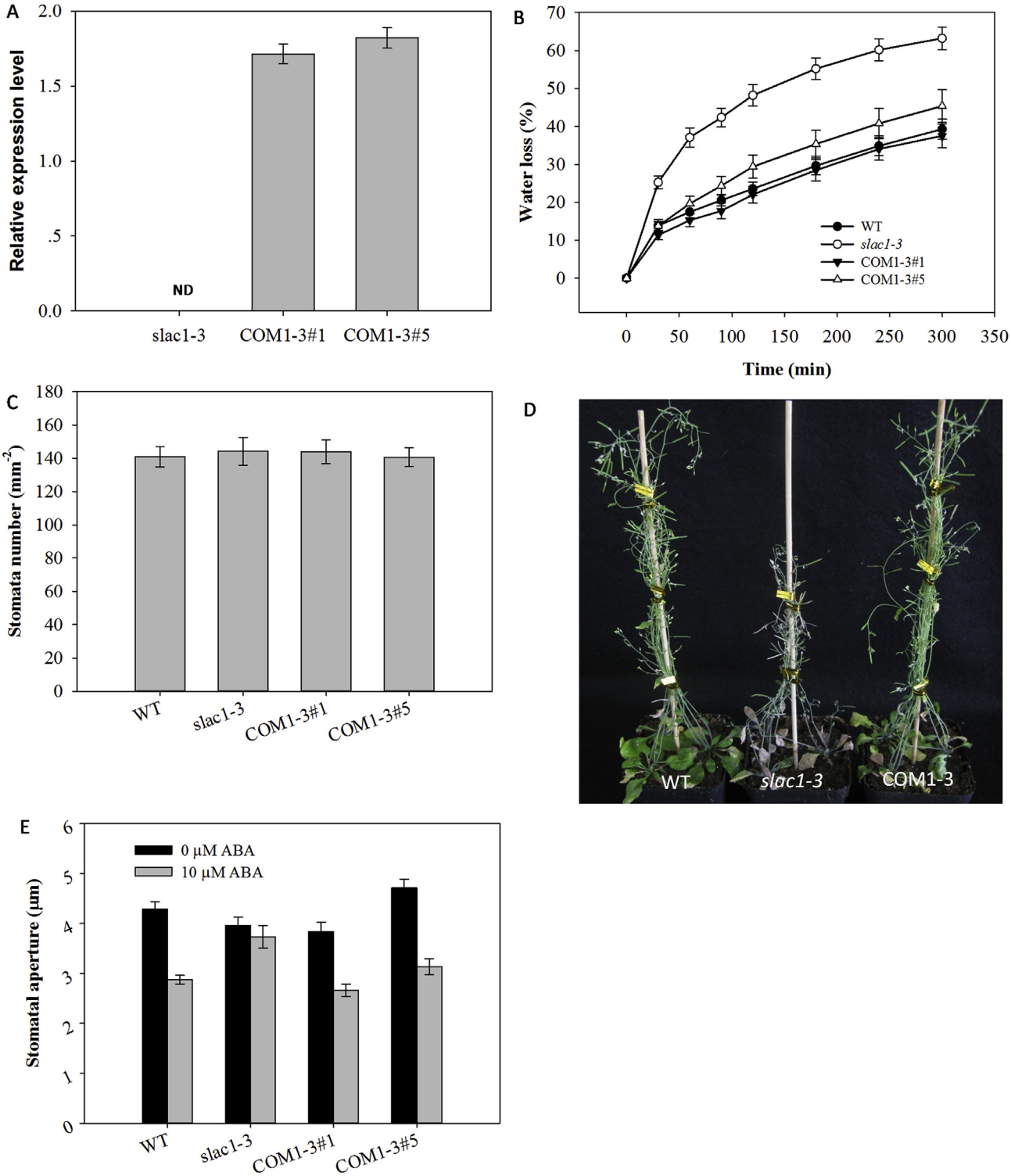

Fig. 5. AmSLAC1 enhances drought tolerance of *slac1-3* mutant in Arabidopsis. (A) Expression level of *AmSLAC1* in the complementation lines. Total RNA was extracted from the rosette leaves of wild-type, *slac1-3* mutants and *slac1/AmSLAC1* complementation lines, and the relative transcript levels of *AmSLAC1* were conducted by qRT-PCR. Bars represent the means of three independent biological replicates ± SE. ND, not detected. (B) Water loss rates from detached leaves of Col-0, *slac1-3* mutants and *slac1/AmSLAC1* complementation lines. Rosette leaves of 4-week-old plants were excised and weighed at the designated time intervals (0, 30, 60, 90, 120, 180, 240, and 300 min after detachment). The water loss rates were calculated as $(W_0\text{-}W_t)/W_0$. Each data point represents the means of three independent biological replicates ± SE (n = 6). (C) Comparisons of stomatal density among 4-week-old wild type, *slac1-3* mutants and *slac1/AmSLAC1* complementation lines. Thirty microscopic sights were observed for each plant, and six plants were used for each genotype. Error bars represent ± SD. (D) Drought tolerance of transgenic plants recovered near the level of wild type. Water was withheld from 4-week-old plants for 2 weeks before the images were taken. The experiments were repeated three times with similar results. (E) The average stomatal aperture of wild type, *slac1-3* mutants and *slac1/AmSLAC1* complementation lines in response to ABA. Error bars represent means ± SD from three independent experiments. At least 120 stomatas were measured for each line per replication.

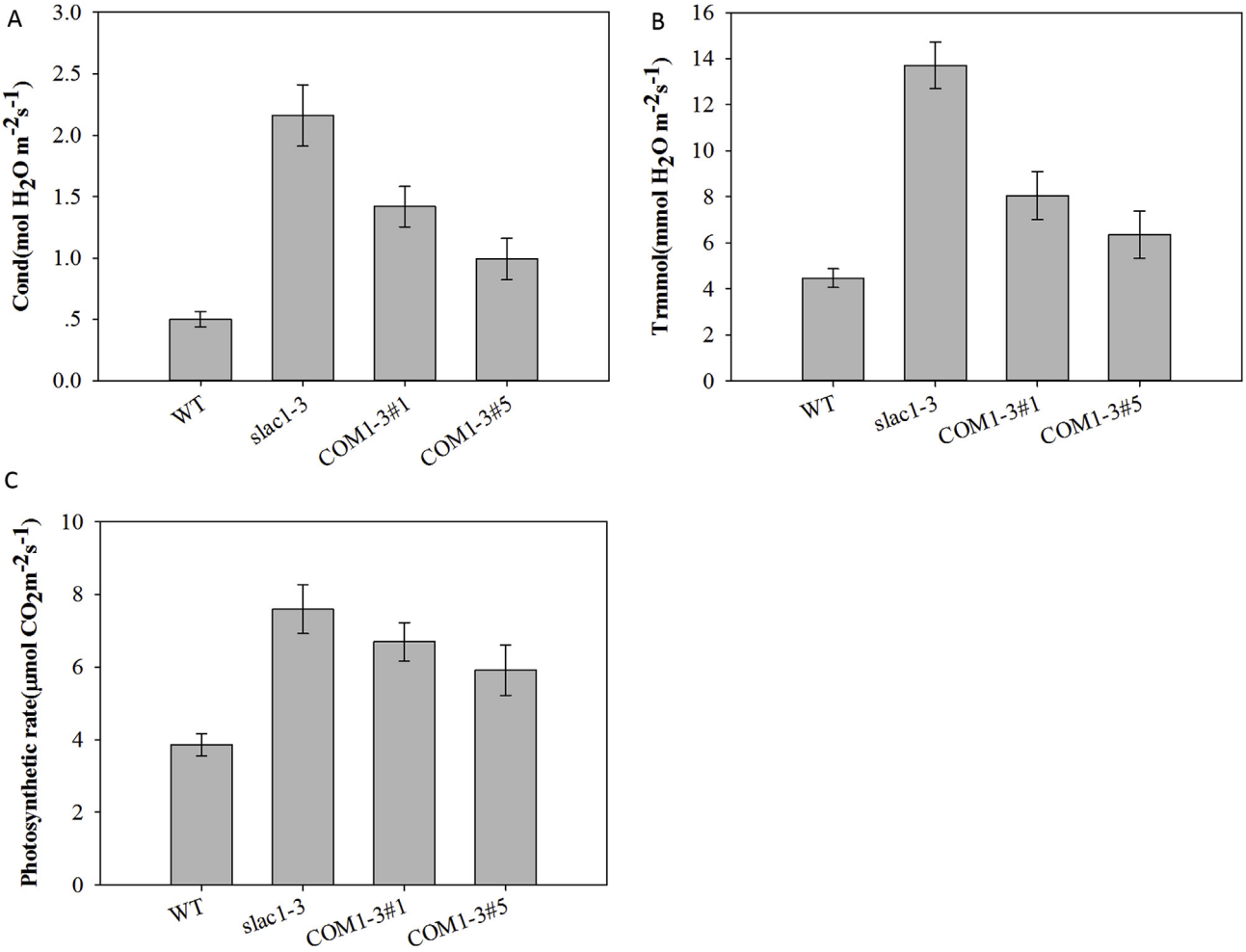

Fig. 6. Photosynthesis characteristic analysis among WT, *slac1-3* mutant and *slac1/AmSLAC1* complementation lines. Comparisons of stomatal conductance (A), transpiration rates (B) and net photosynthetic rate (C) among 4-week-old wild type, *slac1-3* mutants and *slac1/AmSLAC1* complementation lines. Error bars represent ± SD for three independent experiments.

to ABA. As shown in Fig. 5E, the wild-type, *slac1-3* mutants and complementation lines showed a similar stomatal aperture under control conditions. In contrast, when exposed to ABA solution, the *slac1-3* mutants impaired ABA-induced stomatal closure (3.7 μm). And the *AmSLAC1* expressed in *slac1-3* mutants could reduce the size of stomatal pore (2.7 μm in COM1-3#1, 3.1 μm in COM1-3#5) near to the level of the wild type plants (2.9 μm) (Fig. 5E). These results showed that AmSLAC1 took part in stomatal movement and drought tolerance in Arabidopsis.

The size of stomatal aperture is known to determine water and CO_2 exchange; therefore, stomatal conductance, transpiration and photosynthesis were examined by a portable photosynthesis system. Results showed that, as expected, the stomatal conductance and transpiration rate increased in *slac1-3* mutants significantly, and were recovered to the level of the wild type practically in complementation lines (Fig. 6A and B). Interestingly, the photosynthesis rates of complementation lines increased more moderately than that in wild type plants (Fig. 6C).

3.5. Effects of over expression AmSLAC1 on Arabidopsis growth

To examine the effects of over expression *AmSLAC1* on Arabidopsis, we developed transgenic Arabidopsis constitutively to express *AmSLAC1* gene under control of the 35S promoter. Real-time RT-PCR was conducted to detect the transcripts of *AmSLAC1* in their overexpression homozygous plants (Fig. 7A). Two representative homozygote lines (OE#1 and OE#8) with different expression levels were used in the following experiments. No significant differences were detected in excised leaves water loss (Fig. 7B), stomatal aperture (Fig. 7C), stomatal conductance (Fig. 7D), transpiration rates (Fig. 7E) or photosynthetic rates (Fig. 7F) among wild-type and overexpression plants. In addition, no morphological differences were observed after two-week water deficiency between wild-type and overexpression plants (supplemental data). These results indicated that overexpression of *AmSLAC1* in Arabidopsis does not significantly affect stomatal movement and drought tolerance in response to water deficit stress.

3.6. Regulation of AmSLAC1

SLAC1 in Arabidopsis was regulated by protein kinases (Geiger et al., 2009, 2010; Lee et al., 2009). In order to test whether AmSLAC1 could interact with AmCPK6, bimolecular fluorescence complementation (BiFC) experiments were conducted to detect the interaction between AmSLAC1 and AmCPK6 in plant cell. To this end, the corresponding constructs were co-infiltrated into tobacco leaves, as shown in Fig. 8, and distinctive YFP fluorescence signals were observed in the margin of tobacco mesophyll cells.

The two-electrode voltage clamp (TEVC) system was extensively used to measure the ion currents of channels through the membranes of *Xenopus oocytes*. As shown in Fig. 9, oocyte injection with AmSLAC1 or AmCPK6 alone did not induce macroscopic anion currents. However, when coexpressed with AmCPK6, the AmSLAC1 channel currents were apparently activated (Fig. 9A, B and C), indicating that the activity of

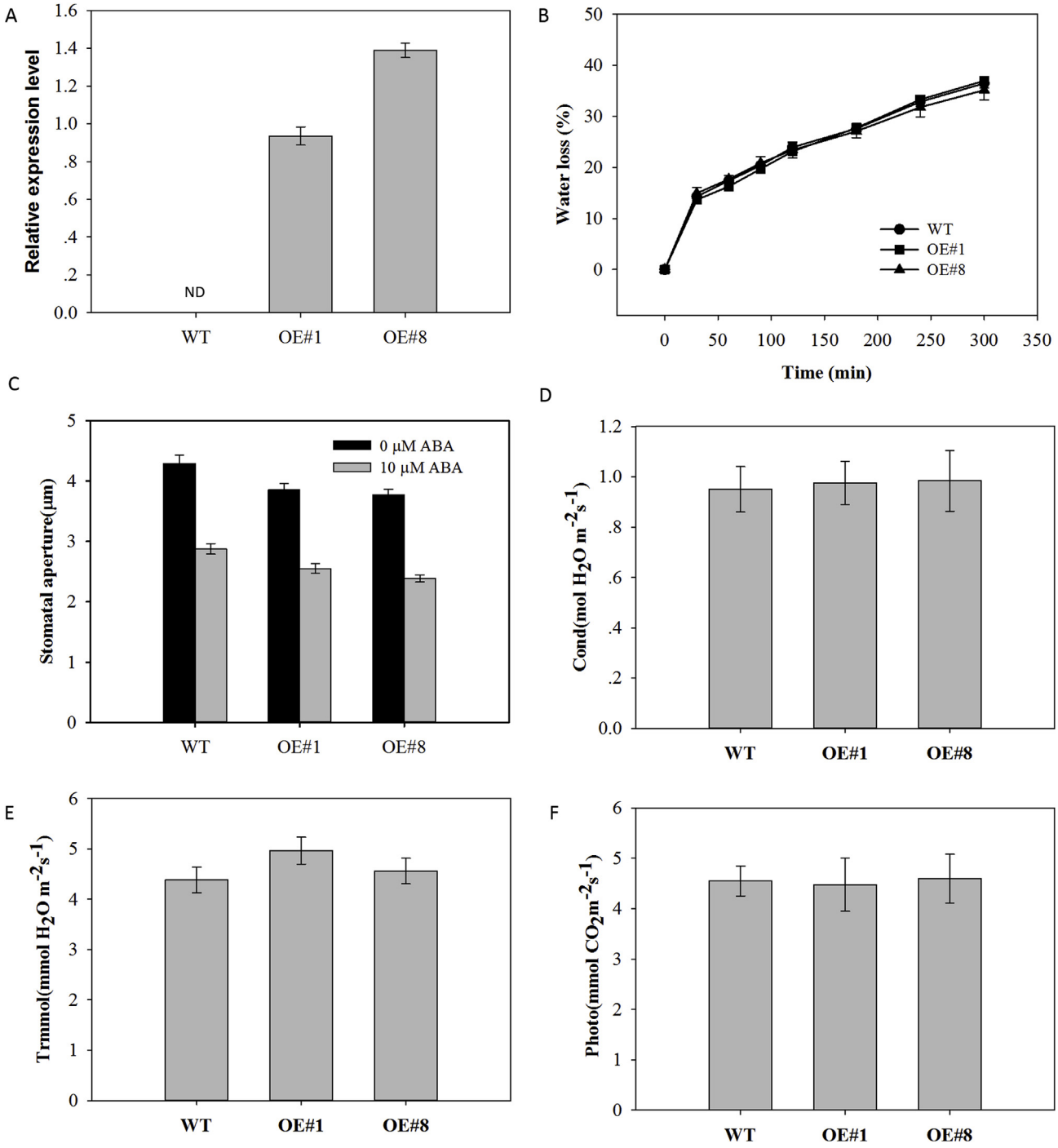

Fig. 7. Effects of *AmSLAC1* overexpression in Arabidopsis. Expression level of *AmSLAC1* in the overexpression lines. Total RNA was extracted from the rosette leaves of wild-type and *AmSLAC1* overexpression lines, and the relative transcript levels of *AmSLAC1* were conducted by qRT-PCR. Bars represent the means of three independent biological replicates ± SE. ND, not detected. (B) Water loss rates from detached leaves of wild-type and *AmSLAC1* overexpression lines. Rosette leaves of 4-week-old plants were excised and weighed at the designated time intervals (0, 30, 60, 90, 120, 180, 240, and 300 min after detachment). The water loss rates were calculated as $(W_0\text{-}W_t)/W_0$. Each data point represents the means of three independent biological replicates ± SE (n = 6). (C) The average stomatal aperture of wild-type and *AmSLAC1* overexpression lines in response to ABA. Error bars represent means ± SD from three independent experiments. At least 120 stomatas were measured for each line per replication. Comparisons of stomatal conductance (D), transpiration rates (E) and net photosynthesis (F) among 4-week-old wild-type and *AmSLAC1* overexpression lines. Error bars represent SD for three independent experiments.

AmSLAC1 channel was largely dependent on the presence of AmCPK6 in oocytes.

4. Discussion

The stomatal complex consists of microscopic pores surrounded by a pair of guard cells found in the epidermis of the leaves. Stomatal aperture is actively regulated by reversible changes that opening and closing is co-ordinated to maintain optimum leaf CO_2 and water potential in guard cell. *Ammopiptanthus mongolicus*, originated from an ancient fabaceous shrub, survives under extreme water deficit and atmospheric dryness for a long historic period, which makes it necessary

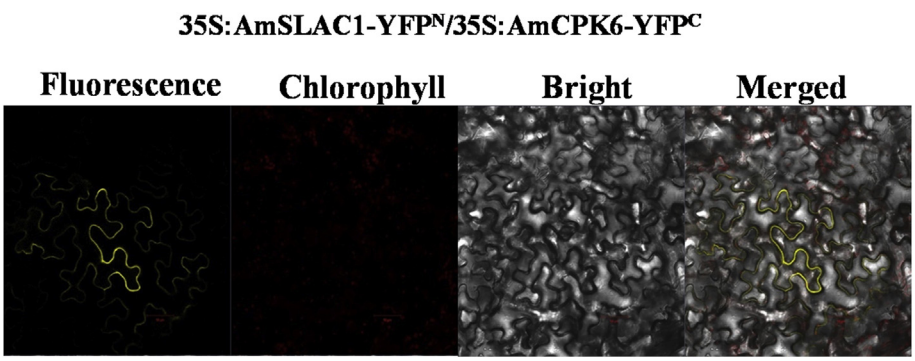

Fig. 8. Interaction analyses of AmSLAC1-AmCPK6. The constructed plasmids were co-transformed into Agrobacterium strain *GV*3101. Pairs of combinations were co-infiltrated in *Nicotiana benthamiana* leaves and analyzed by biomolecular fluorescence complementation (BiFC) assays. At the 48-72nd hr after infiltration, the YFP signal was observed by confocal laser scanning microscopy (Zeiss, LSM710). The results were repeated at least three times.

for this species keeps its stomatal aperture minimum. ABA activates the SLAC-type anion channels along with GORK to facilitate K^+ and Cl^- efflux, and then leads to stomatal closure. Our previous data showed that *Ammopiptanthus mongolicus* GORK showed functional conservation among plant species (Li et al., 2016). However, the contribution of AmSLAC1 to *Ammopiptanthus mongolicus* stomatal movement hasn't been evaluated yet. The present work may further our current knowledge with respect to the isolation and functional character of the putative AmSLAC1.

A putative AmSLAC1 was clone based on our previous RNA-seq data of *Ammopiptanthus mongolicus* (Jin et al., 2018). Phylogenic analysis and sequence alignment showed that AmSLAC1 was highly similar to Arabidopsis and rice SLAC1 (Fig. 1B). According to ProtScale online software (http://web.expasy.org/protscale/), the AmSLAC1 contains 21 phosphorylation sites, including 16 serines, 3 threonines and 2 tyrosines (supplemental data). Amino acid sequences alignment showed that AmSLAC1 contains several phosphorylation sites conservative with that in Arabidopsis, such as S59, S86, S113, and S120 (Geiger et al., 2010; Vahisalu et al., 2010), and were all conserved in rice SLAC1 (Kusumi et al., 2012). In addition, our data showed that AmSLAC1 enabled interaction with AmCPK6 *in vitro* and *in vivo* (Fig. 8B). Furthermore, apparent anion channel conductance mediated by AmSLAC1 was activated by coexpression with AmCPK6 in oocytes (Fig. 9A). In Arabidopsis, the calcium-dependent protein kinases (CPK3, CPK6, CPK21, and CPK23) enabled active SLAC1 in Arabidopsis (Geiger et al., 2010; Brandt et al., 2012). However, in other plant species, similar study has been scarcely reported. In our data, serine 62 (Ser 62) of AmSLAC1 was conservative with that phosphorylating serine 59 (Ser 59) of Arabidopsis SLAC1 (Fig. 1), which is crucial in CPK6 mediated signaling (Brandt et al., 2012). Besides, AmCPK6 interacted with and activated AmSLAC1, resulting in anion channel conductance (Fig. 9A and B).

In accordance with AtSLAC1, the expression of AmSLAC1 was restricted in the shoot of Ammopiptanthus (Fig. 2A). GUS staining of transgenic plants that harbored a Pro-*$_{AmSLAC1}$*::*GUS* construct showed a strong activity in guard cells of leaves (Fig. 2B). Additionally, GUS signals were also detected in trichomes and guard cells of other green parts including hypocotyl and sepal (Fig. 2C, D and H), which was slightly different from that in Arabidopsis (Negi et al., 2008; Vahisalu et al., 2008). In addition, the expression of *AmSLAC1* was upregulated by drought stresses after 24 h treatments (Fig. 2B and C), whereas Arabidopsis SLAC1 was induced rapidly after 3 h drought stress treatment (Zhang et al., 2016). Our previous report showed that the closure of stomata in *Ammopiptanthus* was less sensitive to the induction of ABA (Jin et al., 2018), which may be caused by larger stomata of *Ammopiptanthus* than that of Arabidopsis (Jin et al., 2018), because more ion uptake into or release from guard cell are needed to induce stomatal opening or closing. This might be one reason for delayed in transcript level of *AmSLAC1*in response to drought stresses.

Due to the lack of SLAC1-deficient mutant of *Ammopiptanthus*, expressing *AmSLAC1* in Arabidopsis *slac1-3* mutants were used to determine the physiological roles in plants. The expression of *AmSLAC1* rescued the drought hypersensitive and stomata movement phenotypes of *slac1-3* plants (Fig. 5), indicating AmSLAC1 plays an important role in stomata movement in response to ABA or drought induced stresses. In other plant species, such as in rice, *SLAC1*-deficient mutants showed higher stomatal conductance, rates of photosynthesis, and ratios of internal [CO_2] to ambient [CO_2] compared with wild-type plants (Kusumi et al., 2012). In consistence with Arabidopsis and rice, maize *SLAC1*-deficient mutants *zmslac1-1* and *zmslac1-2* exhibited strong insensitive phenotypes of stomatal closure in response to diverse stimulis (Qi et al., 2018). The expression of *OsSLAC1* in *pAtSLAC1*::*OsSLAC1* transgenic lines rescued the phenotype of *atslac1-3* to drought stress (Sun et al., 2016). Also, ZmSLAC1 was capable of partially rescuing the stomatal movement phenotype of the double mutant *atslac1-3atslac3-2* (Qi et al., 2018). *AmSLAC1* overexpression in Arabidopsis WT resulted in no phenotype under both control and drought stress conditions (Fig. 7 and supplemental data). The expression of *AtSLAC1* was induced in response to PEG treatment in WT plants (supplemental data), containing their own SLAC1 channel, which might be sufficient for closing stomatal when plants suffering water deficiency. All above showed that the function of SLAC1 was conservative among aquatic lived rice, xerophytic grown maize or Arabidopsis, even desert plant *Ammopiptanthus*, indicating that the diversification of SLAC1 might be irrelevant with their growing environment.

Taken together, these results demonstrate that the expression of AmSLAC1 enable complement the phenotypes of Arabidopsis slac1 mutants, indicating that AmSLAC1, as an anion channel and regulated by AmCPK6, is functionally conserved for ABA and drought induced stomata closure.

Conflicts of interest

The authors declare no conflicts of interest.

Authors' contributions

YHS, JLL and HEG designed the work, JLL performed all electrophysiology measurements and partial molecular work, LH prepared plant materials and carried out partial molecular work. JLL, HEG and HCZ wrote the paper. All authors read and approved the manuscript.

Acknowledgments

This work was financially supported through grants from the National Natural Science Foundation of China (grant no. 31601819) and Agricultural scientific and technological innovation project of Shandong Academy of Agricultural Sciences (CXGC2016B10). The authors would like to thank Professor Julian I. Schroeder, Cell and Developmental Biology Section, Division of Biological Sciences, University of California San Diego for providing seeds of Arabidopsis *slac1-3* mutant. Sincere gratitude also goes to Professor Honghong Hu,

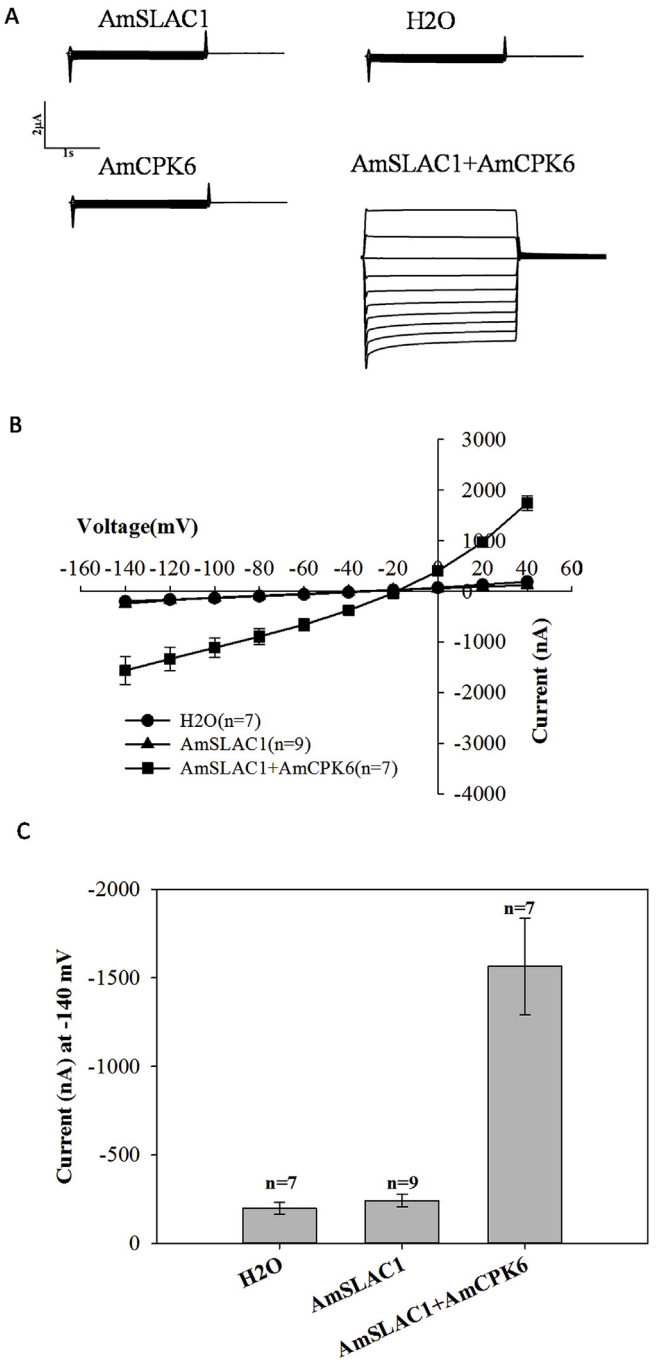

Fig. 9. Regulation of AmSLAC1 by AmCPK6. (A) Typical whole-oocyte anion current recordings with standard bath solution (A), average current-voltage curves of steady-state anion channel currents (B), and the average current amplitudes of instantaneous anion currents at −140 mV (C). The numbers of oocytes tested were seven for control, nine for AmSLAC1, seven for AmSLAC1 + AmCPK6. Error Bars indicate means ± SD.

College of Life Science and Technology, Huazhong Agricultural University for providing Agrobacterium strain *GV*3101 and Professor Yuhai Cui, Agriculture and Agri-Food Canada, Western University for providing the BiFC vectors as gift. We thank Dr. Xun Li, Institute of Soil Science, Chinese Academy of Sciences, for kind assistance in photosynthetic and transpirational assays.

Appendix A. Supplementary data

Supplementary data to this article can be found online at https://doi.org/10.1016/j.plaphy.2019.09.012.

References

Bechtold, U., 2018. Plant life in extreme environments: how do you improve drought tolerance? Front. Plant Sci. 9, 543. https://doi.org/10.3389/fpls.2018.00543.

Bhargava, S., Sawant, K., 2013. Drought stress adaptation: metabolic adjustment and regulation of gene expression. Plant Breed. 132, 21–32.

Brandt, B., Brodsky, D.E., Xue, S., Negi, J., Iba, K., Kangasjarvi, J., Ghassemian, M., Stephan, A.B., Hu, H., Schroeder, J.I., 2012. Reconstitution of abscisic acid activation of SLAC1 anion channel by CPK6 and OST1 kinases and branched ABI1 PP2C phosphatase action. Proc. Natl. Acad. Sci. U. S. A. 109, 10593–10598.

Gao, F., Wang, J.Y., Wei, S.J., Li, Z.L., Wang, N., Li, H.Y., Feng, J.C., Li, H.J., Zhou, Y.J., Zhang, F.X., 2015. Transcriptomic analysis of drought stress responses in *Ammopiptanthus mongolicus* leaves using the RNA-seq technique. PLoS One 10. https://doi.org/10.1371/journal.pone.0124382.

Geiger, D., Scherzer, S., Mumm, P., Marten, I., Ache, P., Matschi, S., Liese, A., Wellmann, C., Al-Rasheid, K.A., Grill, E., Romeis, T., Hedrich, R., 2010. Guard cell anion channel SLAC1 is regulated by CDPK protein kinases with distinct Ca^{2+} affinities. Proc. Natl. Acad. Sci. U. S. A. 107, 8023–8028.

Geiger, D., Scherzer, S., Mumm, P., Stange, A., Marten, I., Bauer, H., Ache, P., Matschi, S., Liese, A., Al-Rasheid, K.A., Romeis, T., Hedrich, R., 2009. Activity of guard cell anion channel SLAC1 is controlled by drought-stress signaling kinase-phosphatase pair. Proc. Natl. Acad. Sci. U. S. A. 106, 21425–21430.

Guzel Deger, A., Scherzer, S., Nuhkat, M., Kedzierska, J., Kollist, H., Brosche, M., Unyayar, S., Boudsocq, M., Hedrich, R., Roelfsema, M.R., 2015. Guard cell SLAC1-type anion channels mediate flagellin-induced stomatal closure. New Phytol. 1, 162–173.

Han, L., Li, J., Jin, M., Su, Y., 2018. Functional analysis of a type 2C protein phosphatase gene from *Ammopiptanthus mongolicus*. Gene 653, 29–42.

Hussain, H.A., Hussain, S., Khaliq, A., Ashraf, U., Anjum, S.A., Men, S., Wang, L., 2018. Chilling and drought stresses in crop plants: implications, cross talk, and potential management opportunities. Front. Plant Sci. 9. https://doi.org/10.3389/fpls.2018.00393.

Jezek, M., Blatt, M.R., 2017. The membrane transport system of the guard cell and its integration for stomatal dynamics. Plant Physiol. 174, 487–519.

Jin, M., Guo, M., Yue, G., Li, J., Yang, S., Zhao, P., Su, Y., 2018. An unusual strategy of stomatal control in the desert shrub *Ammopiptanthus mongolicus*. Plant Physiol. Biochem. 125, 13–26.

Kusumi, K., Hashimura, A., Yamamoto, Y., Negi, J., Iba, K., 2017. Contribution of the S-type anion channel SLAC1 to stomatal control and its dependence on developmental stage in rice. Plant Cell Physiol. 58, 2085–2094.

Kusumi, K., Hirotsuka, S., Kumamaru, T., Iba, K., 2012. Increased leaf photosynthesis caused by elevated stomatal conductance in a rice mutant deficient in SLAC1, a guard cell anion channel protein. J. Exp. Bot. 63, 5635–5644.

Laanemets, K., Wang, Y.F., Lindgren, O., Wu, J., Nishimura, N., Lee, S., Caddell, D., Merilo, E., Brosche, M., Kilk, K., Soomets, U., Kangasjarvi, J., Schroeder, J.I., Kollist, H., 2013. Mutations in the SLAC1 anion channel slow stomatal opening and severely reduce K^+ uptake channel activity via enhanced cytosolic $[Ca^{2+}]$ and increased Ca^{2+} sensitivity of K^+ uptake channels. New Phytol. 197, 88–98.

Lee, S.C., Lan, W.Z., Buchanan, B.B., Luan, S., 2009. A protein kinase-phosphatase pair interacts with an ion channel to regulate ABA signaling in plant guard cells. Proc. Natl. Acad. Sci. U. S. A. 106, 21419–21424.

Li, J.L., Zhang, H.C., Lei, H., Jin, M., Yue, G.Z., Su, Y.H., 2016. Functional identification of a GORK potassium channel from the ancient desert shrub *Ammopiptanthus mongolicus* (Maxim.) Cheng f. Plant Cell Rep. 35, 803–815.

Liu, Y.G., Chen, Y., 2007. High-efficiency thermal asymmetric interlaced PCR for amplification of unknown flanking sequences. Biotechniques 43, 649–650 652, 654.

Negi, J., Matsuda, O., Nagasawa, T., Oba, Y., Takahashi, H., Kawai-Yamada, M., Uchimiya, H., Hashimoto, M., Iba, K., 2008. CO_2 regulator SLAC1 and its homologues are essential for anion homeostasis in plant cells. Nature 452, 483–486.

Qi, G.N., Yao, F.Y., Ren, H.M., Sun, S.J., Tan, Y.Q., Zhang, Z.C., Qiu, B.S., Wang, Y.F., 2018. The S-Type anion channel ZmSLAC1 plays essential roles in stomatal closure by mediating nitrate efflux in Maize. Plant Cell Physiol. 59, 614–623.

Schroeder, J.I., Keller, B.U., 1992. Two types of anion channel currents in guard cells with distinct voltage regulation. Proc. Natl. Acad. Sci. U. S. A. 89, 5025–5029.

Shi, J., Liu, M., Shi, J., Zheng, G., Wang, Y., Wang, J., Chen, Y., Lu, C., Yin, W., 2012. Reference gene selection for qPCR in Ammopiptanthus mongolicus under abiotic stresses and expression analysis of seven ROS-scavenging enzyme genes. Plant Cell Rep. 31, 1245–1254.

Sun, S.J., Qi, G.N., Gao, Q.F., Wang, H.Q., Yao, F.Y., Hussain, J., Wang, Y.F., 2016. Protein kinase OsSAPK8 functions as an essential activator of S-type anion channel OsSLAC1, which is nitrate-selective in rice. Planta 243, 489–500.

Vahisalu, T., Kollist, H., Wang, Y.F., Nishimura, N., Chan, W.Y., Valerio, G., Lamminmaki, A., Brosche, M., Moldau, H., Desikan, R., Schroeder, J.I., Kangasjarvi, J., 2008. SLAC1 is required for plant guard cell S-type anion channel function in stomatal signalling. Nature 452, 487–491.

Vahisalu, T., Puzorjova, I., Brosche, M., Valk, E., Lepiku, M., Moldau, H., Pechter, P., Wang, Y.S., Lindgren, O., Salojarvi, J., Loog, M., Kangasjarvi, J., Kollist, H., 2010. Ozone-triggered rapid stomatal response involves the production of reactive oxygen species, and is controlled by SLAC1 and OST1. Plant J. 62, 442–453.

Zhang, A., Ren, H.M., Tan, Y.Q., Qi, G.N., Yao, F.Y., Wu, G.L., Yang, L.W., Hussain, J., Sun, S.J., Wang, Y.F., 2016. S-type Anion channels SLAC1 and SLAH3 function as essential negative regulators of inward K^+ channels and stomatal opening in Arabidopsis. Plant Cell. https://doi.org/10.1105/tpc.16.01050.

Zoulias, N., Harrison, E.L., Casson, S.A., Gray, J.E., 2018. Molecular control of stomatal development. Biochem. J. 475, 441–454.